STU SjF

Strojnícky časopis – Journal of MECHANICAL ENGINEERING,
VOL 76 (2026), NO 2, 1 – 10

EXPERIMENTAL MEASUREMENT AND ESTIMATION OF VEHICLE LATERAL DYNAMICS PARAMETERS USING MULTI-SENSOR DATA

BACH Sebastian[1], MILESICH Tomáš[1], DANKO Ján[1*], KEVICKÝ Igor[1], BÉREŠ Marko[1], BERNÁTH Martin[1], MAGDOLEN Ľuboš[1]

[1] Slovak University of Technology in Bratislava, Faculty of Mechanical Engineering, Institute of Automotive Engineering and Designs, Nám. slobody 17,812 31 Bratislava, Slovakia, e – mail: jan.danko@stuba.sk*

Abstract: This paper presents an experimental evaluation of vehicle lateral dynamics using multi-sensor data and a linear bicycle model. The measured signals are synchronized, filtered and transformed to the vehicle centre of gravity. Vehicle and axle slip angles, lateral forces and axle cornering stiffness are determined. The estimated stiffness varies during the manoeuvre and is therefore interpreted as a local effective parameter rather than a constant vehicle property.

Keywords: vehicle lateral dynamics, bicycle model, sideslip angle, lateral force, cornering stiffness, experimental measurement

1 Introduction

Vehicle lateral dynamics is an important area of vehicle engineering, as it directly affects vehicle stability, handling and safety during cornering and transient manoeuvres. The lateral motion of a vehicle is primarily governed by the interaction between the tyres and the road surface and by the resulting lateral forces. Important quantities describing this behaviour include lateral acceleration, yaw rate, vehicle sideslip angle, axle slip angles and cornering stiffness [1–3].

The experimental determination of these quantities is challenging because some of them cannot be measured directly and must therefore be derived from other measured signals. For this purpose, experimental data can be combined with a mathematical model of the vehicle. One of the most commonly used simplified approaches is the single-track, or bicycle, model, in which the left and right wheels of each axle are replaced by an equivalent wheel. Despite its simplicity, the model retains the fundamental relationships between vehicle motion, steering input and lateral tyre forces and is particularly suitable for the analysis of vehicle behaviour at relatively small slip angles [1, 2].

The aim of this paper is to experimentally evaluate the lateral dynamics of a passenger vehicle and to estimate selected dynamic parameters using data obtained from multiple measurement systems. The measured signals are synchronized, filtered and transformed to the vehicle centre of gravity. Based on the processed data and a linear bicycle model, the vehicle sideslip angle, front and rear axle slip angles and lateral forces are determined. These quantities are subsequently used to estimate the effective cornering stiffness of the front and rear axles and to evaluate its behaviour during the analysed driving manoeuvre.

2 Vehicle model and parameter estimation method

The lateral motion of the vehicle is described using a linear single-track, or bicycle, model. In this model, the left and right wheels of each axle are replaced by one equivalent wheel located

DOI: 10.2478/scjme-2026-0018, Print ISSN 0039-2472, On-line ISSN 2450-5471
© This is an open access article licensed under the Creative Commons Attribution-NonCommercial-NoDerivatives License (http://creativecommons.org/licenses/by-nc-nd/4.0/).

at the centre of the corresponding axle. A schematic representation of the bicycle model used in this study is shown in Fig. 1. The vehicle motion is considered in the horizontal plane and is described by the longitudinal velocity v_x, lateral velocity v_y, and yaw rate r. The distances of the vehicle centre of gravity from the front and rear axles are denoted by l_f and l_r, respectively [1, 2].

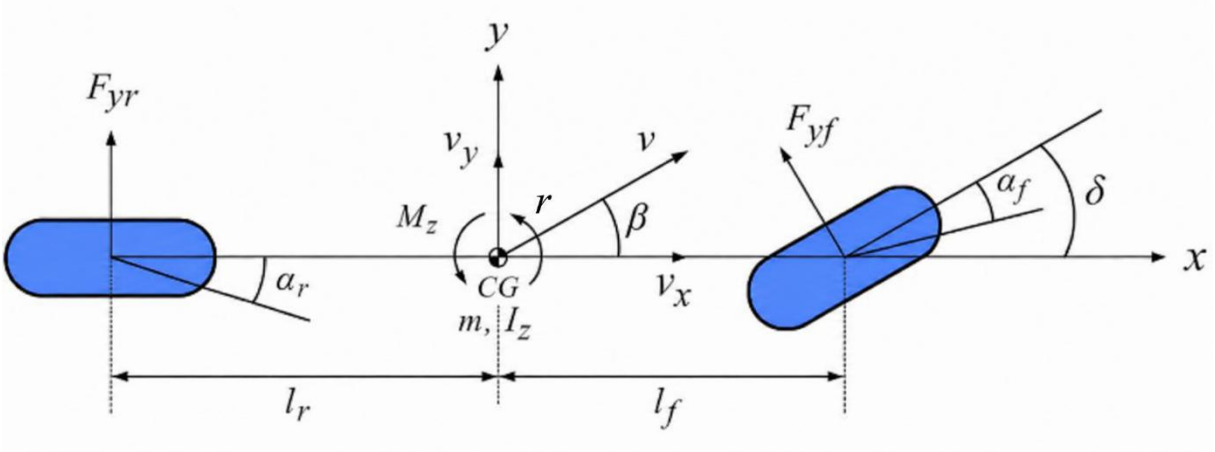


Fig. 1 Single-track bicycle model of the vehicle [4].

The vehicle sideslip angle β, defined as the angle between the velocity vector at the vehicle centre of gravity and the longitudinal vehicle axis, is determined as [1]:

$$\beta = arctan\left(\frac{v_y}{v_x}\right). \tag{1}$$

Based on the bicycle model, the slip angles of the front and rear axles are calculated according to [1, 2]:

$$\alpha_f = \delta_f - \beta - \frac{l_f r}{v_x}, \tag{2}$$

$$\alpha_r = -\beta + \frac{l_r r}{v_x}, \tag{3}$$

where δ_f is the steering angle of the front wheels. These quantities represent the angular difference between the orientation of the equivalent axle wheel and its actual direction of motion. The same relations are used in the experimental evaluation of the measured manoeuvre.

The total lateral force acting on the vehicle is obtained from the measured lateral acceleration a_y and the vehicle mass m:

$$F_y = ma_y. \tag{4}$$

For subsequent parameter estimation, the total lateral force is divided between the front and rear axles by considering both lateral force equilibrium and moment equilibrium about the vertical axis of the vehicle. The corresponding axle forces are expressed as [1, 2]:

$$F_{yf} = \frac{l_r F_y + I_z \dot{r}}{l}, \tag{5}$$

$$F_{yr} = \frac{l_f F_y - I_z \dot{r}}{l}, \tag{6}$$

here I_z is the yaw moment of inertia, $\dot{r}$ is the yaw acceleration and $l = l_f + l_r$ is the wheelbase.

For relatively small slip angles, the relationship between lateral force and slip angle can be approximated by a linear tyre model [2, 3]. For the front and rear axles, respectively, this relationship is written as

$$F_{yf} = C_f \alpha_f,\ F_{yr} = C_r \alpha_r, \tag{7}$$

where C_f and C_r represent the effective cornering stiffness of the front and rear axles. The cornering stiffness parameters are estimated locally from the relationships $F_{yf}(\alpha_f)$ and $F_{yr}(\alpha_r)$ within a moving time window. Data points corresponding to very low vehicle speed, lateral force or slip angle are excluded to reduce the influence of numerically unstable and physically insignificant values.

The linear relationship in Eq. (7) is primarily applicable in the region of small slip angles. Under real operating conditions, the lateral tyre force is also influenced by vertical load, road adhesion and the current operating point of the tyre [2, 3]. Therefore, the estimated values of C_f and C_r are interpreted as effective parameters representative of the analysed driving manoeuvre rather than constant properties of the tyres or axles.

3 Experimental setup of the test vehicle and measurement systems

The experimental measurements were carried out using a Peugeot 208 passenger vehicle in its standard production configuration, without modifications to the suspension or steering system. The measurements were performed on a closed test area at the Slovakia Ring, allowing driving manoeuvres with repeated changes of direction to be carried out safely. During the measurements, the vehicle was occupied by the driver and equipped with the required measurement systems.

The basic vehicle parameters required for the lateral dynamics model are summarized in Tab. 1. The total vehicle mass and the longitudinal position of the centre of gravity were determined experimentally from individual wheel loads. The yaw moment of inertia was not measured directly. The radius of gyration about the vertical axis was assumed as $k_z \approx 0.5l$, resulting in the estimate $I_z = 0.25ml^2 \approx 1987\ \mathrm{kg\,m^2}$. This value is treated as an estimated model parameter.

The experimental setup consisted of several independent measurement systems, since no single sensor provided all quantities required for the subsequent analysis. Vehicle velocity components were measured using a CORREVIT S-350 Aqua optical sensor, which provides contactless measurement of vehicle motion relative to the road surface [5]. An Xsens MTi-670 GNSS/INS unit was used to record the vehicle yaw rate and accelerations [6]. Vehicle position and trajectory were obtained using a u-blox C102-F9R GNSS receiver [7]. The steering wheel angle was measured using a Nidec RE30E-1000-213-1 incremental optical encoder mounted on the steering column [8]. The encoder signal was subsequently converted into the steering wheel angle and used to determine the front wheel steering angle. The main measured quantities used in the analysis are summarized in Tab. 2.

The test vehicle equipped with the measurement systems is shown in Fig. 2. The signals obtained from the individual systems were recorded independently and therefore required subsequent synchronization and signal processing before being used for the estimation of the lateral dynamics parameters.

Tab. 1 Basic parameters of the test vehicle

Parameter	Value
Vehicle mass, m	1232.5 kg
Wheelbase, l	2.54 m
CG distance from front axle, lf	0.94 m
CG distance from rear axle, lr	1.60 m
Yaw moment of inertia, Iz	≈ 1987 kg·m²

Tab. 2 Measurement systems and quantities used in the analysis

Measurement system	Quantities used
CORREVIT S-350 Aqua	longitudinal and lateral velocity, local sideslip angle
Xsens MTi-670 GNSS/INS	yaw rate, longitudinal and lateral acceleration
u-blox C102-F9R	vehicle position and velocity
Nidec RE30E-1000-213-1	steering wheel angle

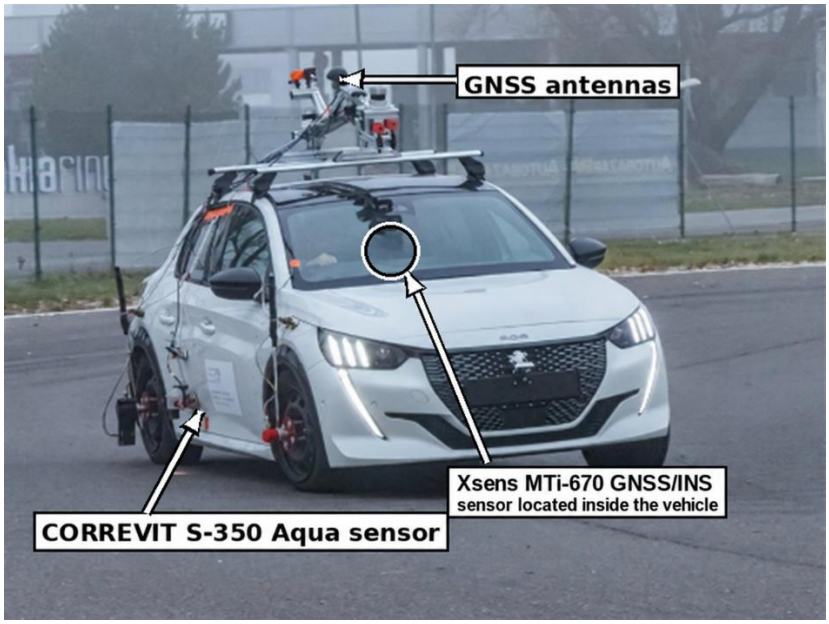


Fig. 2 Test vehicle equipped with the measurement systems.

Detailed views of the measurement equipment installed in the test vehicle are shown in Fig. 3 and Fig. 4.

4 Data processing

The measured data were processed in MATLAB before their use in the vehicle model. Since the individual measurement systems did not share a common time base, their signals were first synchronized. The time shift between the GNSS/INS and CORREVIT data was determined by maximizing the correlation between the vehicle velocity signals measured independently by both systems [9]. The measured signals were subsequently smoothed using a moving-average

filter. Zero-phase filtering was applied to avoid introducing an additional time delay, particularly for yaw rate, acceleration, steering angle and velocity signals [9, 10].

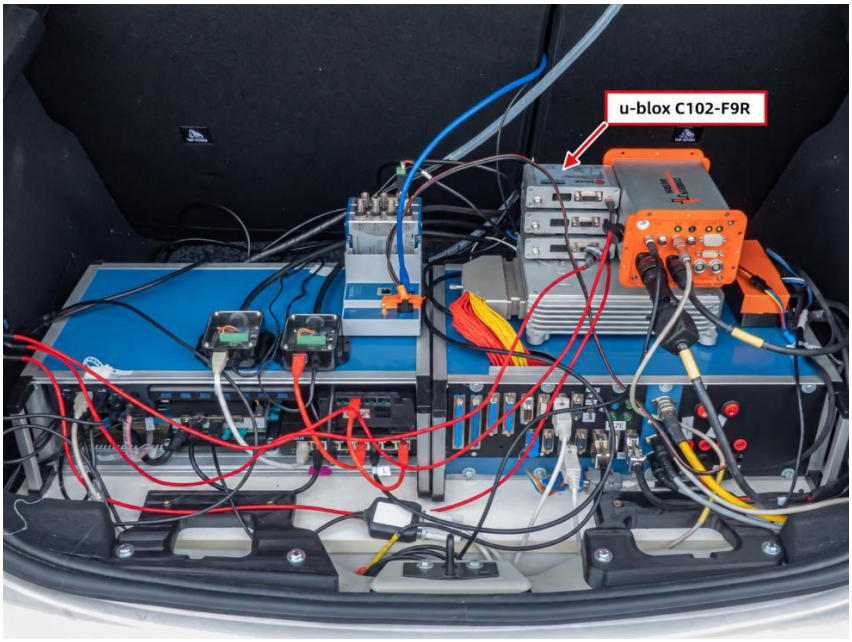


Fig. 3 Data-acquisition equipment and u-blox C102-F9R GNSS receiver installed in the luggage compartment of the test vehicle.



Fig. 4 Nidec RE30E-1000-213-1 encoder installed on the steering column for steering wheel angle measurement.

The steering wheel angle was obtained from the incremental encoder signal after correcting its zero offset and converting the measured pulses to angular displacement. The steering ratio was determined experimentally from a separate test run with approximately steady-state cornering. The front wheel steering angle was estimated from the bicycle model and the steering

ratio was calculated as the ratio between the steering wheel and front wheel angles. Its final value was determined as the median over the selected steady-state interval to reduce the influence of noise and outliers [9], resulting in a steering ratio of approximately $i = 14.15$.

Because the CORREVIT sensor was mounted outside the vehicle centre of gravity, its measured velocity components had to be transformed to the centre of gravity before evaluating the lateral dynamics. For planar vehicle motion, the transformation is given by [1, 2]

$$v_{x,CG} = v_{x,corr} + r\, y_{corr,CG}, \tag{8}$$

$$v_{y,CG} = v_{y,corr} - r\, x_{corr,CG}, \tag{9}$$

where $x_{corr,CG}$ and $y_{corr,CG}$ describe the sensor position relative to the vehicle centre of gravity. This transformation removes the contribution of vehicle yaw motion at the sensor location and provides the velocity components required for the calculation of vehicle sideslip and axle slip angles.

5 Results and discussion

The main analysis was performed using test run No. 11, which was selected because it provided sufficient lateral excitation of the vehicle and suitable data quality for synchronization of the individual measurement systems. The complete run was not evaluated; instead, a selected section containing repeated changes of direction and sufficiently pronounced lateral dynamics was used for the parameter estimation.

The velocity components transformed to the vehicle centre of gravity were first used to determine the vehicle sideslip angle. As shown in Fig. 5, the sideslip angle β remained predominantly within approximately $-2°$ to $2°$ during most of the analysed manoeuvre. Short-term peaks of up to approximately $\pm 5°$ occurred towards the end of the selected interval, where the manoeuvre became more dynamic. The relatively small sideslip angle over most of the interval is favourable for the application of the simplified bicycle model, while the higher short-term values indicate operating conditions in which nonlinear vehicle and tyre behaviour may become more significant [1–3].

Since the vehicle sideslip angle enters directly into the calculation of the front and rear axle slip angles, its accuracy is important for the subsequent parameter estimation. Errors in the transformed velocity components would therefore propagate into the estimated slip angles and, consequently, into the effective cornering stiffness.

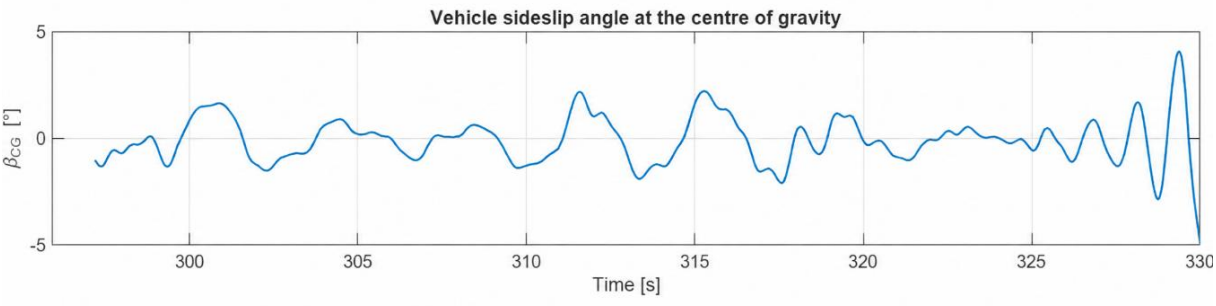


Fig. 5 Vehicle sideslip angle during the analysed manoeuvre.

The calculated front and rear axle slip angles are presented in Fig. 6. A clear difference between the behaviour of the two axles can be observed. The front axle slip angle α_f reaches approximately $-13°$ to $13°$, whereas the rear axle slip angle α_r remains predominantly within approximately $-5°$ to $5°$. The larger values at the front axle are related to the direct influence

of the front wheel steering angle, while the rear axle slip angle results mainly from the lateral velocity and yaw motion of the vehicle [1, 2].

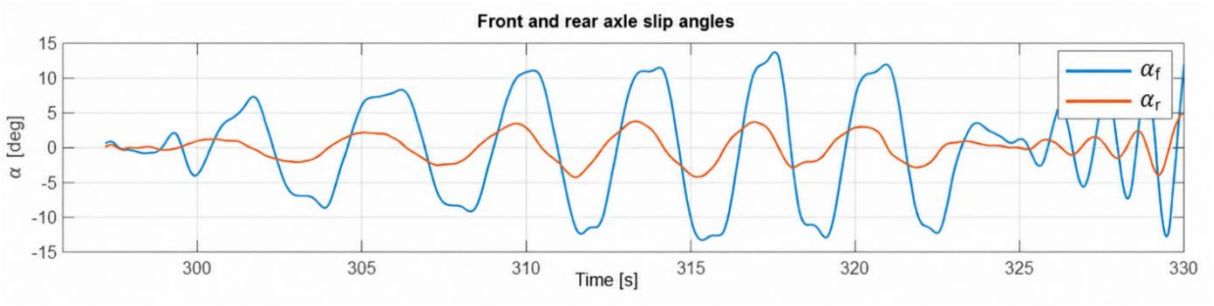


Fig. 6 Front and rear axle slip angles during the analysed manoeuvre.

The magnitude of the front axle slip angle is particularly important when interpreting the subsequent cornering stiffness estimation. The linear tyre model assumes an approximately proportional relationship between lateral force and slip angle, which is mainly applicable at relatively small slip angles. At higher values, the actual tyre characteristic becomes nonlinear and the increase in lateral force is no longer directly proportional to the slip angle [3]. Previous simulation-based research has shown that vehicle stability during cornering is strongly influenced by the tyre–road adhesion coefficient and the available lateral force at the wheels [11]. Therefore, especially during the portions of the manoeuvre with higher α_f, the estimated stiffness should not be interpreted as a constant tyre parameter.

The total lateral force calculated from the measured lateral acceleration follows the alternating character of the driving manoeuvre, with repeated changes of sign corresponding to successive changes in the direction of vehicle motion. Peak values reach approximately $\pm 1.2 \times 10^4$ N, confirming that the selected manoeuvre provides sufficiently strong lateral excitation for further evaluation of the vehicle dynamics.

For the estimation of the axle parameters, the total lateral force was divided into the front and rear axle forces F_{yf} and F_{yr}. Their time histories are shown in Fig. 7. Both forces follow a similar general trend to the total lateral force, while their individual magnitudes vary according to the yaw dynamics of the vehicle. In particular, the term containing the yaw acceleration and yaw moment of inertia affects the instantaneous distribution of the lateral force between the axles [1, 2].

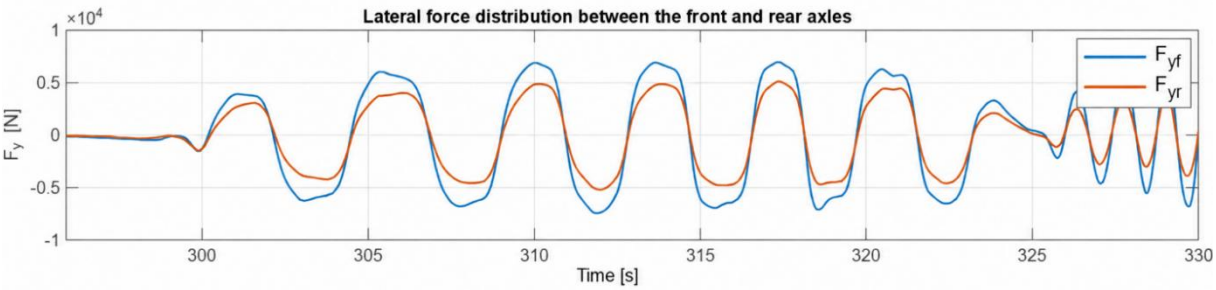


Fig. 7 Lateral forces acting on the front and rear axles during the analysed manoeuvre.

The interpretation of the calculated axle forces must also take into account the uncertainty of the yaw moment of inertia. Since I_z was not measured experimentally but estimated from the vehicle mass and wheelbase, the calculated F_{yf} and F_{yr} represent model-based estimates rather than directly measured axle forces. The uncertainty of I_z propagates through the term $I_z\dot{r}$ and consequently affects the subsequent estimation of the axle cornering stiffness.

The effective cornering stiffness of the front and rear axles was estimated locally from the relationships between axle lateral force and the corresponding slip angle. Instead of calculating

an instantaneous ratio F_y/α, the parameters C_f and C_r were estimated within a moving time window. Values corresponding to very low vehicle speed, lateral force or slip angle were excluded to reduce the influence of numerically unstable and physically insignificant operating points. The resulting time histories are presented in Fig. 8.

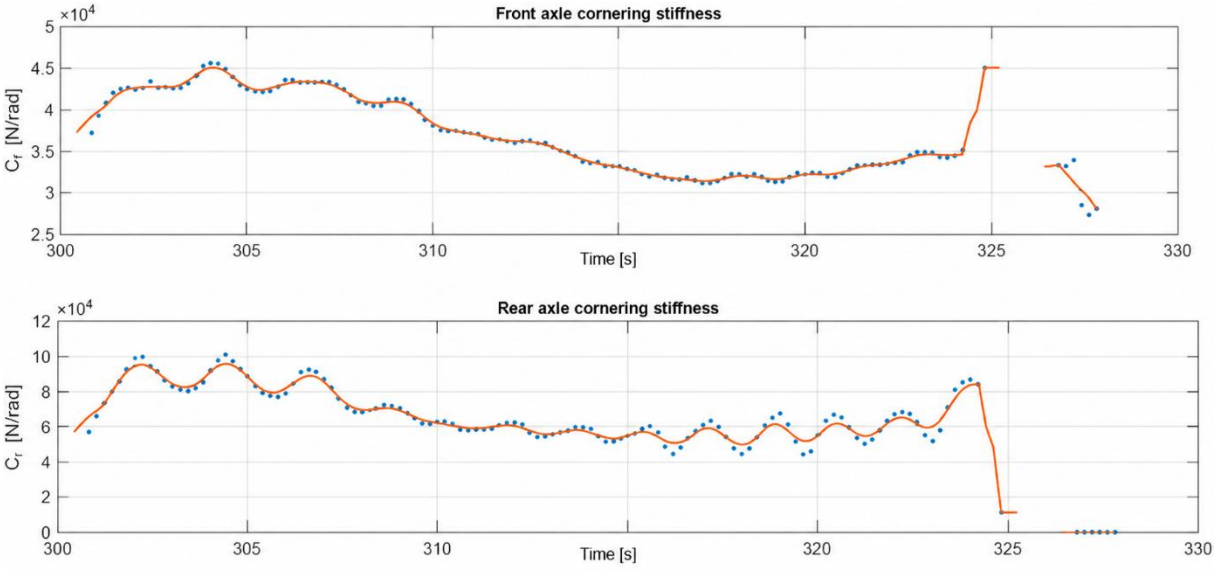


Fig. 8 Estimated effective cornering stiffness of the front and rear axles.

The estimated values of C_f and C_r are not constant throughout the analysed manoeuvre. This behaviour should not be interpreted simply as a change in an intrinsic tyre property. Rather, the obtained parameters represent the effective axle cornering stiffness resulting from the combination of real vehicle behaviour, measured signals and the simplified mathematical model.

Several effects contribute to the observed variation. First, the tyre force characteristic becomes nonlinear as the slip angle increases [3]. Second, the lateral force generated by a tyre also depends on its vertical load. During cornering, lateral acceleration produces load transfer between the inner and outer wheels, which changes the operating conditions of the tyres and therefore influences the resulting axle lateral force [2, 3]. The single-track model replaces the left and right wheels of each axle with one equivalent wheel and therefore does not explicitly describe lateral load transfer or vehicle roll. Their effects can nevertheless appear indirectly in the experimentally estimated parameters.

Additional uncertainty is introduced by the measurement and signal-processing chain. The calculated quantities depend on the quality and synchronization of the measured signals, the applied filtering, and particularly the numerical derivative of yaw rate required for the calculation of yaw acceleration. Filtering can modify both the amplitude and the dynamic response of measured quantities, while differentiation tends to amplify measurement noise [10]. The approximate value of the yaw moment of inertia represents another significant source of uncertainty because it directly influences the calculated distribution of lateral force between the axles. Related inverse multibody simulation research has similarly shown that unmeasured tyre forces and slip-related quantities can be reconstructed from experimental vehicle data, while the reliability of the results strongly depends on sensor calibration, synchronization, data quality and model accuracy [12].

Overall, the results demonstrate that the combination of multi-sensor experimental measurements and a simplified single-track model can provide a consistent description of the main quantities governing vehicle lateral dynamics. Vehicle sideslip, axle slip angles and lateral

forces can be obtained from the processed measurements and subsequently used for the estimation of axle cornering stiffness. However, due to the nonlinear behaviour observed at higher slip angles, load-transfer effects, uncertainty of the vehicle parameters and limitations of the measured data, the resulting C_f and C_r values should be regarded as local estimates of effective cornering stiffness for the analysed manoeuvre rather than fixed parameters of the vehicle.

CONCLUSION

This paper presented an experimental approach for evaluating vehicle lateral dynamics using data from several measurement systems combined with a linear bicycle model. After synchronization, filtering and transformation of the measured signals to the vehicle centre of gravity, the vehicle sideslip angle, axle slip angles and lateral forces were determined.

The processed data were subsequently used to estimate the effective cornering stiffness of the front and rear axles. The estimated values varied during the analysed manoeuvre, indicating the influence of tyre nonlinearity, changing operating conditions and the simplifications of the applied model. Therefore, the obtained C_f and C_r values should be interpreted as local effective parameters rather than constant vehicle properties.

The proposed methodology demonstrates that meaningful lateral-dynamics parameters can be estimated from experimental vehicle measurements. Further improvement could be achieved by more accurate determination of the yaw moment of inertia and by using a nonlinear tyre model.

ACKNOWLEDGEMENT

This research was supported by the Slovak Research and Development Agency under Contract No. APVV-24-0526 and APVV-23-0650.

REFERENCES

[1] Rajamani, R. "Vehicle Dynamics and Control", 2nd ed., Springer, New York, USA, **2012**. DOI: 10.1007/978-1-4614-1433-9

[2] Gillespie, T. D. "Fundamentals of Vehicle Dynamics", SAE International, Warrendale, USA, **1992**. DOI: 10.4271/R-114

[3] Pacejka, H. B. "Tire and Vehicle Dynamics", 3rd ed., Butterworth-Heinemann, Oxford, UK, **2012**. DOI: 10.1016/C2010-0-68548-8

[4] Li, P., Nguyen, A.-T., Du, H., Wang, Y., Zhang, H. "Polytopic LPV approaches for intelligent automotive systems: State of the art and future challenges", Mechanical Systems and Signal Processing, 161, 107931, **2021**. DOI: 10.1016/j.ymssp.2021.107931

[5] Kistler Group. "Correvit S-350 – Non-Contact Optical Sensors, Type CS350A", Kistler Group, Winterthur, Switzerland, Doc. CS350A_000-807e-03.12, **2012**.

[6] Movella. "MTi-670 GNSS/INS", [online] Available at: https://www.xsens.com/sensor-modules/xsens-mti-670-gnss-ins [Accessed: 13 September **2026**].

[7] u-blox AG. "C102-F9R Application Board – User Guide", u-blox AG, Thalwil, Switzerland, Doc. UBX-20029244, Rev. R04, **2023**. Available at: https://content.u-blox.com/sites/default/files/documents/C102-F9R_UserGuide_UBX-20029244.pdf.

[8] Nidec Components Corporation. "RE30E Optical Encoders", [online] Available at: https://www.nidec-components.com/e/catalog/rotary-encoder/re30e.pdf [Accessed: 13 September **2026**].

[9] Montgomery, D. C., Runger, G. C. "Applied Statistics and Probability for Engineers", 7th ed., John Wiley & Sons, Hoboken, USA, **2018**. ISBN 978-1-119-40030-1

[10] Oppenheim, A. V., Willsky, A. S., Nawab, S. H. "Signals and Systems", 2nd ed., Prentice Hall, Upper Saddle River, USA, **1997**. ISBN 978-0-13-814757-0

[11] Magdolen, Ľ., Danko, J., Milesich, T., Kevický, I., Hanko, L., Skyrčák, R. "Conditions for Loss of Stability of an Autonomous Vehicle During a Cornering Manoeuvre", Strojnícky časopis – Journal of Mechanical Engineering 72 (3), pp. 129 – 140, **2022**. DOI: 10.2478/scjme-2022-0047

[12] Tobiáš, M., Straka, T., Porteš, P. "Inverse Multibody Simulations for Motorcycle Tire Force Analysis", Strojnícky časopis – Journal of Mechanical Engineering 74 (1), pp. 159 – 168, **2024**. DOI: 10.2478/scjme-2024-0016.